RSC Advances

PAPER

View Article Online
View Journal | View Issue



Cite this: *RSC Adv.*, 2020, **10**, 5827

# Mechanical and physicochemical behavior of a 3D hydrogel scaffold during cell growth and proliferation†

Rebeca E. Rivero,‡§[ab] Virginia Capella,‡[ab] A. Cecilia Liaudat,[b] Pablo Bosch,[b] Cesar A. Barbero,[a] Nancy Rodríguez[b] and Claudia R. Rivarola *[a]

Some of the essential properties for cellular scaffolding are the capability to maintain the three-dimensional (3D) structure, good adhesion, and adequate elastic modulus during cell growth, migration, and proliferation. Biocompatible synthetic hydrogels are commonly used as cellular scaffolds because they can mimic the natural extracellular matrices (ECMs). However, it is possible that the physicochemical and mechanical behavior of the scaffold changes during cell proliferation and loses the scaffold properties but this is rarely monitored. In this work, the physicochemical and mechanical properties of a macroporous soft material based on poly(*N*-isopropyl acrylamide) (PNIPAM) have been studied during a period of 75 days at culture condition while bovine fetal fibroblasts (BFF) were grown within the matrix. The interconnected macroporous hydrogel was obtained by cryogelation at −18 °C. The swelling capacity of the scaffold was not altered during cell proliferation but changes in the mechanical properties were observed, beginning with the high elastic modulus (280 kPa) that progressively decreased until mechanical stability (40 kPa) was achieved after 20 culture days. It was observed that the matrix–cell interactions together with collagen production favor normal cellular processes such as cell morphology, adhesion, migration, and proliferation. Therefore, the observed behavior of macroporous PNIPAM as a 3D scaffold during cell growth indicates that the soft matrix is cytocompatible for a long time and preserves the suitable properties that can be applied in tissue engineering and regenerative medicine.

Received 8th October 2019
Accepted 20th January 2020

DOI: 10.1039/c9ra08162c

rsc.li/rsc-advances



## Introduction

Hydrogels are hydrated polymeric networks with diverse properties that have, in recent years, allowed major advancements in their design, fabrication, and applications. The areas of use range from cell and therapeutic delivery to *in vitro* or *in vivo* platforms for creating and controlling cellular environments.[1,2]

Biomaterials based on natural and synthetic hydrogels are being widely used to develop cell-laden scaffolds or *in vitro* tissue-like structures analogous to extracellular membranes (ECMs). Hydrogels have great potential in tissue engineering because they can simulate the mechanical and physiological features of *in vivo* tissues. They can emulate the extracellular matrix structure, providing sites for adhesion, proliferation, and ultimately cell differentiation.[3,4]

Hydrogels have the advantage that they can be synthesized with the required physiological properties by modifying the chemical structure or composition of the starting materials, density of linking of polymer chains, elasticity, or porosity according to the particular biomedical application.[5]

Some important factors to consider in scaffold design include biocompatibility, cell adhesion, proliferation, and differentiation.[6] While there are many chemical approaches for designing scaffolds, we chose poly(*N*-isopropylacrylamide) (PNIPAM) in our work. PNIPAM is one of the most widely used synthetic polymers for biomedical applications due to its volume phase transition temperature of about 32 °C, which is close to the normal human body temperature, and its proven biocompatibility.[7–11] The biocompatibility of PNIPAM in contact with BFFs,[12] human epithelial colorectal adenocarcinoma cells

[a]*Chemistry Department, Faculty of Exact, Physical-Chemical and Natural Sciences, Institute of Research in Energy Technologies and Advanced Materials (IITEMA), National University of Rio Cuarto (UNRC)-National Council of Scientific and Technical Research (CONICET), National Route 36 KM 601, X5804ZAB Rio Cuarto, Cordoba, Argentina. E-mail: crivarola@exa.unrc.edu.ar; Fax: +54 358 4680280; +54 358 4676233; +54 358 4676224; Tel: +54 358 4676157 (5)*

[b]*Molecular Biology Department, Faculty of Exact, Physical Chemical and Natural Sciences, Institute of Environmental Biotechnology and Health (INBIAS), National University of Rio Cuarto (UNRC)-National Council of Scientific and Technical Research (CONICET), National Route 36 KM 601, X5804ZAB Rio Cuarto, Cordoba, Argentina*

† Electronic supplementary information (ESI) available. See DOI: 10.1039/c9ra08162c

‡ These authors contributed equally to this work.

§ Present address: Department of Complex Tissue Regeneration, MERLN Institute for Technology-Inspired Regenerative Medicine, Maastricht University, 6211 LK Maastricht, The Netherlands.

(Caco-2) and lung cancer cells (Calu-3),[13] mesenchymal stem cells derived from rat bone marrow (BM-MSCs), human adipose tissue (AT-MSCs),[14] smooth muscle (SMC),[15] and other biological systems has been demonstrated. In addition, the cytotoxicity of PNIPAM and bioadhesive properties of murine preadipose cells (3T3-L1), human embryonic kidney cells (HEK293), and human carcinoma-derived cells (A549) in contact with these surfaces were recently studied.[16] In many cases, swollen hydrogels can be extremely weak materials and exhibit poor mechanical properties,[17] thus limiting their utilization as three-dimensional matrices.[18] However, there are several strategies to increase the material elastic modulus[19] including semi-interpenetrated systems,[20] polymeric nanocomposite formation,[21,22] co-polymerization,[23] modification of the monomer/crosslinker ratio,[24] and the incorporation of rod-like pores.[25] Previous works have demonstrated that the time-varying mechanical properties (viscoelasticity) of synthetic ECMs can alter the cellular mechanotransduction processes. Thereby, it has been demonstrated that viscoelastic synthetic ECMs mimic the cellular microenvironments more closely.[26]

Hydrogels have recently gained significant interest in the field of 3D tissue engineering and *in vitro* cell culture techniques due to their inherent interconnected porous structure and the relative simplicity of porous micrometer size formation.[27] The intrinsic porosity (nanopores) of hydrogels allows the diffusion of biological flows but its size is not big enough to allow cell proliferation/migration inside the material. Although a macroporous scaffold would allow cell growth inside the matrix, this could weaken its mechanical properties. In the last few years, we have been successful in increasing the porosity and Young's modulus of PNIPAM hydrogel through the synthesis based on the cryogelation of NIPAM at sub-zero temperatures in the presence of a crosslinker and the initiator system.[25]

To the best of our knowledge, research works studying the changes in the mechanical properties of 3D scaffold materials during cell culture do not exist. Therefore, this work is focused on the study of mechanical, physicochemical, and biological behaviour of the cell-scaffold system during several culture days of BFF, which are used as model cells.

Cytotoxicity was analysed by MTT and Neutral Red staining assays. Cellular distribution inside the scaffold was followed through cell nuclei fluorescence staining with Hoechst 33258. Confocal microscopy confirmed cell proliferation inside the 3D scaffold and the presence of collagen over the matrix was observed by the Picrosirius polarization (PSR-POL) method. Cell adhesion was analysed by bright-field optical microscopy. Regarding the mechanical properties of the 3D matrix, a significant decrease in the elastic modulus value was observed during the first days and then, after 40 culture days, a slight increase, probably due to cell growth and collagen production, was observed. The initial observed change in the Young's modulus of the scaffold could be due to a fast relaxation exhibited by the macroporous hydrogel, which then remains stable for a long duration during cellular growth. Therefore, the observed results suggest that the PNIPAM scaffold is highly biocompatible for 3D cell culture since it preserves the mechanical properties and the cell proliferation, adhesion, and migration can progress for more than 75 culture days.

## Experimental methods

### Materials

Hydrogels were synthesized *via* free radical polymerization of *N*-isopropylacrylamide (NIPAM) (Sigma-Aldrich). *N*,*N*-Methylenebisacrylamide (BIS) (Sigma-Aldrich) was used as the crosslinking agent. Ammonium persulfate (APS) (Sigma-Aldrich) and *N*,*N*,*N*′,*N*′-tetramethylenediamine (TEMED) (Sigma-Aldrich) were employed as the initiator system. The reaction mechanism of hydrogel formation is described in the ESI (Scheme S1).†

### Synthesis of macroporous PNIPAM hydrogel scaffold

Crosslinking agent, BIS (2% moles based on NIPAM moles) and APS (0.001 g $mL^{-1}$) were dissolved in an aqueous solution of NIPAM monomer (0.5 M). The pre-polymeric solution was kept at 0 °C. Then, TEMED (10 μL $mL^{-1}$) was added, and the solution was transferred to a 1 mL plastic syringe and sealed immediately. The loaded syringe was placed in an expanded polystyrene tubular box, where it fits tightly, with one of its extremes open and the other closed to allow unidirectional cooling (Scheme 1). This system was placed in a freezer set at −18 °C and kept undisturbed. After 24 h of reaction, complete conversion was achieved. Then, the contents of the syringe were thawed at room temperature and the wet hydrogel was thoroughly washed with deionized water to remove the unreacted chemicals.[25]

### Physicochemical and mechanical characterization of the hydrogel scaffold

**Fourier transform infrared spectroscopy (FTIR).** FTIR spectra were recorded on a Nicolet Impact 400 spectrometer (Nicolet Instrument Corporation, Madison, Wis. USA) by

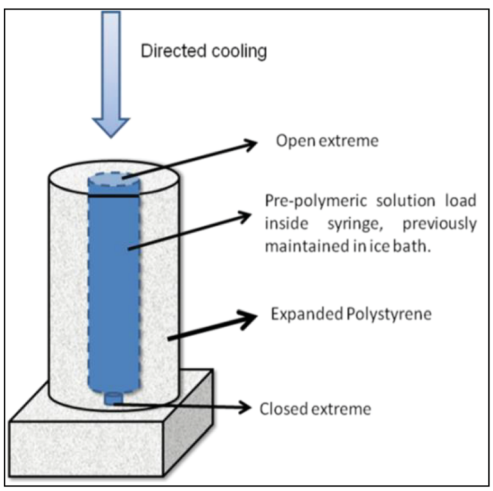


Scheme 1 Representation of the device by polymerization with directed cooling at −18 °C.

 

transmission. The dry hydrogel was crushed and mixed with dry KBr salt to form pills under pressure and vacuum.

**Differential scanning calorimetry (DSC).** Differential scanning calorimetry measurements were used to determine the phase transition temperature of the thermosensitive hydrogel. The measurements were conducted using a DSC 2010, purchased from TA Instruments, under $N_2$ flow. Sealed aluminium capsules were quickly cooled in the calorimeter chamber at −25 °C by filling the outer reservoir with a frozen solution of $CaCl_2$ in water (80% w/w). After several minutes, the system reached the equilibrium state. The sample holder assembly was then heated to 60 °C (above the phase transition temperature) at a rate of 10 °C $min^{-1}$. The temperature was maintained below 100 °C to avoid sample water evaporation.

**Scaffold swelling percentage.** Hydrogel samples, previously washed and dried, were weighed and then placed in complete cell culture medium, DMEM/FBS (DMEM Invitrogen, with 10% v/v of fetal bovine serum (FBS)), at 37.0 ± 0.5 °C. The swelling experiments were carried out at the defined cell culture days.

Each sample was removed from the culture medium at days 0, 14, 22, 45, and 75, weighed, and then the equilibrium swelling percentage was calculated as:

$$\%\ \mathrm{Sw(eq)} = [(W_{eq} - W_{dry})/W_{dry}] \times 100 \quad (1)$$

where $W_{eq}$ represents the weight of the hydrogel at the defined culture day and $W_{dry}$ is the weight of the dry hydrogel determined before the experiment begins. % Sw(eq) at day zero was determined by considering $W$(eq) after 24 h of swelling without the cells.[5] Equilibrium swelling percentage (% Sw(eq)) represents the maximum capacity of the hydrogel to absorb the solution at a defined temperature. % Sw(eq) values were obtained by averaging five measurements.

**Analysis of hydrogel morphology.** The hydrogel morphology was analysed by using scanning electron microscopy (SEM) and optical microscopy. The samples were examined in a LEO 1450VP variable field emission SEM. To perform this method, the samples were previously freeze-dried and then covered with a thin layer of gold by sputtering (2 min at 15 mA). In addition, the freeze-dried samples were observed by an inverted optical microscope (Nikon Ti-S 100, Nikon Japan) and the photographs were taken using a digital camera (Nikon, Japan).

**Elastic modulus ($E$) determination by uniaxial compression.** The elastic modulus of an object is the slope of the stress–strain curve in the elastic deformation region.[28] Details about the performance of the device (used to determination of $E$) and used equations have been previously described[29] and are represented in Scheme 2. A cylindrical hydrogel piece of approximately 0.5 cm diameter and 1–1.5 cm height was placed on an analytical digital balance (OHAUS Pioneer, readability and reproducibility of 0.1 mg). Then, a force ($F = m \times g$) was applied on the hydrogel through a micrometric actuator ($m$ is the read mass and $g$ is the acceleration due to gravity). The stress $\varepsilon$ was calculated as $F/A$, where $A$ is the transverse area of the cylinder. The resulting deformation was measured using a digital comparator (Schwyz electronic indicators). The length changes in the comparator were measured before ($L_1$) and after ($L_2$) the application of force, and $\Delta L$ was calculated as their difference ($L_2 - L_1$). $L_0$ was measured using an absolute micrometer and the strain was calculated as $\sigma = \Delta L/L_0$. The force and the resulting deformation were recorded after 30 seconds of relaxation. During the measurements, the load was increased in successive steps until the hydrogel was deformed up to about 10% compression. By plotting $\varepsilon$ against $\sigma$, it is possible to calculate the Young's modulus ($E$) from the slope.

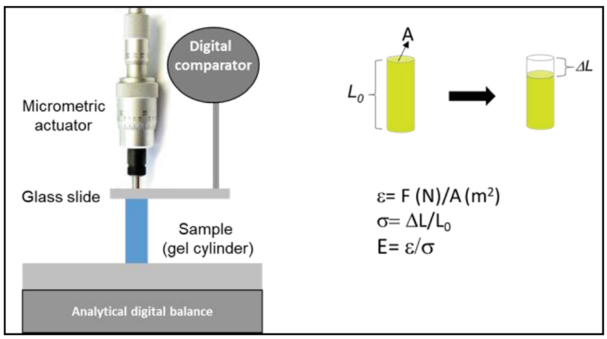


Scheme 2 Description of the device used to determine the elastic modulus.

Uniaxial compression was applied on individual cylindrical hydrogels swollen in the equilibrium state in the culture medium. Keeping the hydrogel at 37 °C in our device during the determination of $E$ was not possible; therefore, it was proposed to simulate the swelling state of the collapsed hydrogel. For this, during culture, the hydrogel was left at 37.0 ± 0.5 °C in the culture medium until its collapsed equilibrium state; after the removal and equilibration at room temperature, the elastic modulus was measured. In this way, the hydrogel contains the amount of liquid corresponding to the collapsed state. All the samples were treated equally to simulate the same conditions. At the same time, the elastic modulus was measured without and with cells inside the 3D macroporous hydrogel at different days of culture. The experiments were performed thrice and the results were averaged.

## Biological experiments

**Seeding method of bovine fetal fibroblasts (BFF).** BFF cells, modified to constitutively express a green fluorescent protein (GFP) (generously provided by Dr Wilfried Kues, Friedrich Loeffler Institute, Germany), were used to perform the experiments.[30] BFF were cultured in Dulbecco's modified Eagle's medium (DMEM) supplemented with 10% (v/v) fetal bovine serum (FBS) and 1% (v/v) antibiotic-antimycotic (penicillin–streptomycin–fungizone, Gibco). Cells passaged at 80–85% confluence and were used after passage for all the experiments.

Macroporous PNIPAM cylinders were employed as 3D scaffold matrices with the following dimensions: 5.5 mm (cylinder diameter) and 9.5 mm (tube length) at 22.0 °C. Two days prior to cell seeding, the 3D scaffolds were sterilized in 70% ethanol overnight.[31] The ethanol was removed by collapsing the hydrogels and washing them with PBS (phosphate saline buffer, pH

7.4) for 30 min three times. After that, the matrices were washed twice for 30 min in PBS supplemented with 10% v/v antibiotic-antimycotic. To remove traces of antibiotic-antimycotic, the hydrogels were washed anew with PBS, as previously described. The hydrogels were collapsed and rehydrated (swollen) with complete cell culture medium (DMEM, 10% fetal bovine serum (FBS), and 1% antibiotic-antimitotic) overnight and placed at the well bottom of a 24-well plate with complete DMEM/FBS medium. On the next day, BFFs were seeded onto macroporous hydrogels at a density of $10^5$ cells per well, as shown in Scheme 3, and incubated at 37 °C under 5% $CO_2$ humidified atmosphere for 75 days.[12]

**Viability assays.** To evaluate the material cytotoxicity, two assays were carried out-MTT and Neutral Red uptake (NR). MTT assay is often used to determine the cytotoxicity following exposure to toxic substances. MTT (3-[4,5-dimethylthiazol-2-yl]-2,5-diphenyltetrazolium bromide) is a water-soluble tetrazolium salt, which is converted to insoluble purple formazan by the cleavage of the tetrazolium ring by succinate dehydrogenase mitochondrial enzyme. The formazan product is impermeable to the cell membranes and therefore, it accumulates in healthy cells.[32] The Neutral Red uptake assay is also used to measure the cell viability. It is based on the ability of viable cells to incorporate and bind the supravital dye Neutral Red in the lysosomes.[33,34]

Briefly, BFFs were seeded in 96-well plates at $5 \times 10^3$ cells per well in 200 μL of complete DMEM/FBS. After one day, a piece of the hydrogel was placed in contact with the cells and then incubated for 24 h at 37 °C in a humidified atmosphere of 5% $CO_2$. After this, the hydrogel piece was removed and MTT or NR solution was added.

MTT reagent (1 mg $mL^{-1}$) was added to each well and further incubated for 3 h at 37 °C. The reaction mixture was removed from each well, replaced by 100 μL of dimethyl sulfoxide (DMSO), and the optical density (OD) was measured at 540 nm using a microplate reader (Bio-Rad). Each experimental condition included a viability control group in which the hydrogel was omitted. The viable cell number after 24 h of culture was expressed as OD of formazan obtained for each hydrogel and control group.

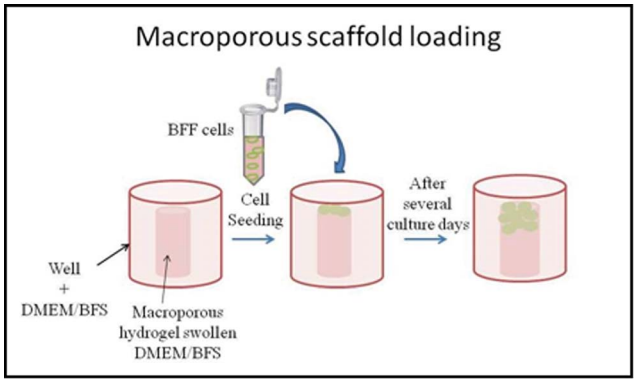


Scheme 3 Load process of macroporous PNIPAM scaffold with BFF cells.

For the NR assay, 1 μg $mL^{-1}$ of NR was added to the cells and the cell control, which were incubated for 3 h. After incubation, the solution was removed, the wells were washed, and NR desorption solution (49 parts of water, 50 parts of ethanol, 1 part of acetic acid, freshly prepared) was added to all the wells. The plates were shaken for 30 minutes and thereafter, the absorbance was measured at 540 nm in the same way as the MTT assay.

**Cell nuclei distribution and morphology.** To analyse the cell nuclei distribution inside the hydrogel matrix, Hoechst 33258 nuclear staining technique was used. The cells inside the PNIPAM macroporous hydrogel were fixed with methanol at −20 °C at least 12 h before the staining and then small pills were cut. 100 μL of Hoechst 33258 (100 μg $mL^{-1}$)[35] was added to cover the pieces for 15 minutes. After that, the pills were washed with PBS and were observed by inverted fluorescence microscopy under UV light (filter range: excitation 360 ± 40 nm and fluorescence emission 460 ± 50 nm).

The images of a small piece of hydrogel with cells expressing a green fluorescent protein (GFP) grown inside it were acquired by confocal laser scanning microscopy (Olympus FV 1200) to analyse the cell morphology.

Both types of fluorescence, Hoechst and GFP, were observed on the same sample, in order to verify the cell growth.

**Picrosirius red polarization method for the determination of collagen (PSR-POL).** Sample analysis was carried out following the protocol of histological assessments. Portions of approximately 6 $mm^3$ of hydrogel scaffolds after 14, 22, 43, and 75 days of culture were fixed by immersion in 10% (v/v) buffered-saline formaldehyde pH 7.2–7.4 at 4 °C, dehydrated with alcohol, and embedded in paraffin. Then, the pieces were cut in ≈5 μm histological sections with a microtome (Micron, Germany) and mounted on slides.

Paraffin-embedded sections (5 μm thick) were deparaffinised through xylene and a graded alcohol series, and then stained for 30 minutes with Picrosirius Red (0.1% of Sirius Red in saturated aqueous picric acid), as described by Junqueira *et al.*[36] for collagen bundle detection. Sections were then mounted for observation under polarized light microscopy (Nikon Labophot-Pol).

**Statistical analysis.** Data were analysed using ANOVA with INFOSTAT/L program. Post-hoc comparisons were performed using Bonferroni's test. The values are expressed as means ± SE and $p < 0.05$ was considered statistically significant.

## Results and discussion

### Characterization and morphology of the 3D macroporous scaffold

Macroporous PNIPAM hydrogels were synthesized *via* cryopolymerization. Unidirectional cooling at −18 °C allows the use of water crystals as template of rod-like macropores.

The FTIR spectrum shows the characteristics bands of functional groups of PNIPAM. An intense band in the range of 3700–3000 $cm^{-1}$ corresponding to N–H signal of secondary amides and amides associated and 2800–3000 $cm^{-1}$ of C–H

 

stretching can be seen. The N–H stretching bands of amide I and II appear at ~1660 and 1518 $cm^{-1}$ and the isopropyl methyl deformation bands at 1386 and 1367 $cm^{-1}$ (ESI, Fig. S1†).[17]

In addition, characteristic phase transition temperature was determined by DSC at ~33.7 °C in water and at 33.9 °C in the culture medium (ESI, Fig. S2†), which corresponded to the bibliographic dates.[5]

Thin films of hydrogel cylinder were cut to analyse the morphology by optical microscopy and SEM.

In order to verify the presence of longitudinal pores, cuts at parallel and transversal directions to the major axis of the cylinder hydrogel were made. Optical microscopy image of lyophilized hydrogel shows, in Fig. 1A, the spherical pores separated by hydrogel thin walls (thin black zones) while Fig. 1B shows the longitudinal rod-like pores.

A freeze-dried piece of hydrogel was covered with gold to be analysed by SEM. Fig. 1C and D show the images of transversal cuts where macropores have diameters of about 100 μm. Besides, macroporous walls also have micropores of about 5 to 20 μm diameter, which interconnect the macropores.

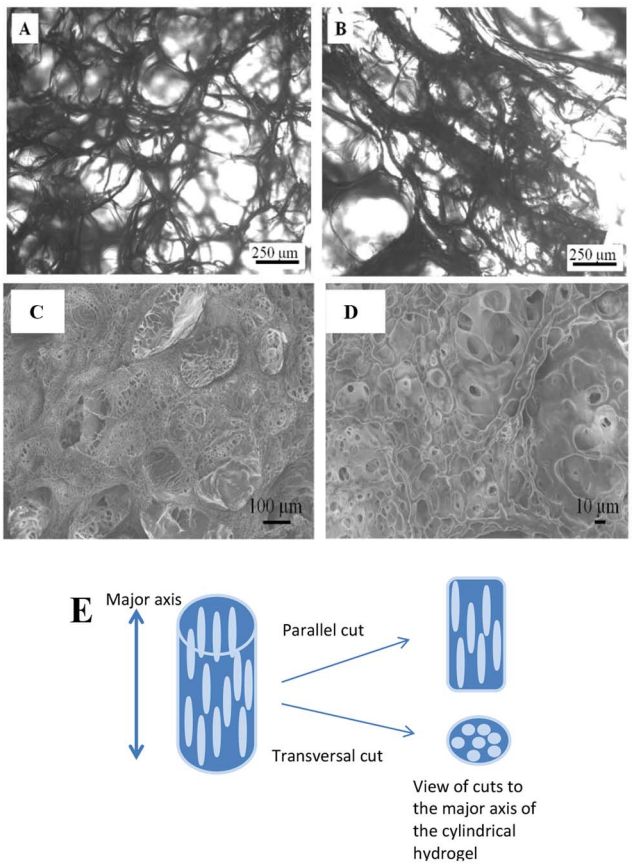


Fig. 1 Images of hydrogels synthesized by cryogelation obtained by optical microscopy: (A) transversal cut and (B) parallel cut to the major axis of the cylindrical hydrogel. (C and D) SEM images of the PNIPAM hydrogel synthesized by cryogelation on transversal cut to the major axis of the cylindrical hydrogel at different scales. (E) Representation of the 3D macroporous matrix structure and transversal and parallel cuts' view.

Both the microscopies confirm that longitudinal and interconnected pores inside the hydrogel are obtained by unidirectional cryopolymerization.[25,37]

Previous studies have demonstrated that pore sizes of 5–15 μm are optimum for fibroblast growth and 100–350 μm for bone regeneration, while pore sizes of 500 μm are required for vascularization and fibrovascular tissue growth.[38] In this way, the material studied in this work has the porosity and microarchitecture required to be used as 3D scaffold, allowing the free flow of biological fluids and cell migration and growth inside the material.

## Cytotoxicity assays and cell distribution

The cytotoxicity assays were performed in order to verify the viability of BFF cells in contact with the 3D PNIPAM scaffold. So, two different assays were performed: MTT and Neutral Red. MTT assay indicates the healthy cell number by the accumulation of formazan inside the cell cytoplasm while Neutral Red is accumulated inside the functional lysosomes. The optical density of the corresponding dyes was followed at 540 nm for both assays after 24 h of BFFs, which are shown in Fig. 2A. The OD differences between the negative control (polystyrene) and the cells in contact with the PNIPAM scaffold are compared and no significant differences are observed, indicating the absence of toxicity.

On the other hand, Hoechst staining assay gives information about cell distribution inside the matrix. Hoechst 33258 ($C_{25}H_{26}N_6OH$) is a fluorescent molecule permeable to the cell bilayer that binds to the DNA of live cells, which can be easily followed by inverted fluorescence microscopy. In Fig. 2B, a great number of fluorescent points corresponding to fluorescent cell nuclei can be seen. A homogenous distribution was observed in the PNIPAM scaffold after 40 culture days. The same distribution was observed later by confocal laser scanning microscopy.

## 3D cell proliferation by confocal laser scanning microscopy

Cells expressing GFP allow us to follow the 3D cell growth during several culture days by confocal laser scanning microscopy. In addition, Hoechst staining enables us to recognize viable cells, by comparison of merged images. The scanned area corresponds to 497.64 microns (axis $z$) and 635.205 × 635.205 microns (axis $x$ and $y$) where 429 slides are merged.

After 40 culture days, it can be seen in Fig. 2C that the green zones corresponding to the GFP-cell adhered to the hydrogel walls unlike the black zones that correspond to empty pores. These images confirm that BFFs penetrate the scaffold, adhere to the hydrogel walls, and grow inside the macroporous matrix. Noteworthly, BFF cells are not stained; these were chemically modified to constitutively express a green fluorescent protein, which is a part of the genomic sequence of cellular ADN. Therefore, the hydrogel cannot be stained by the cells.

Similar images were observed after Hoechst staining (Fig. 2D), where the high density of the fluorescent nuclei did not allow the clear observation of the isolated cell nucleus. The overlapping

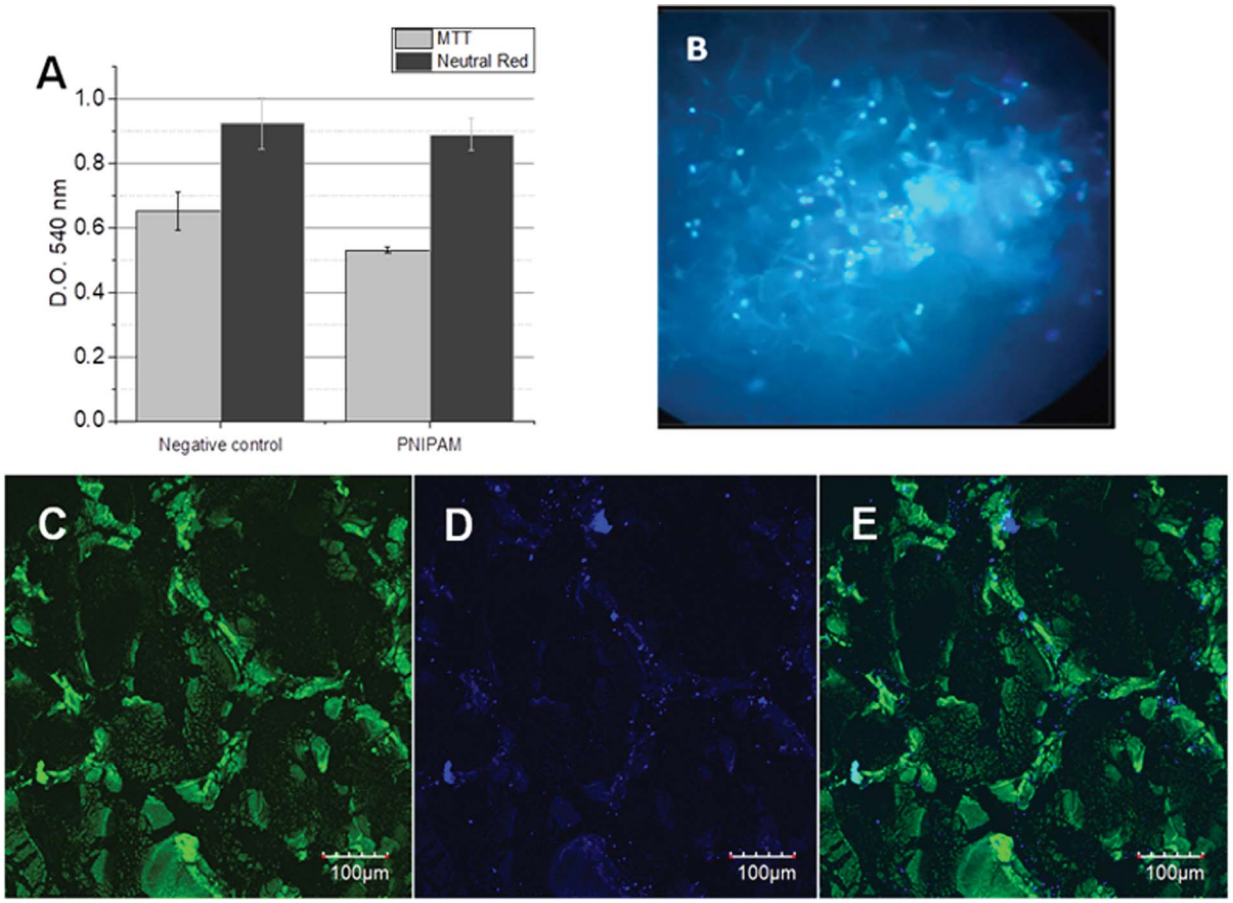


Fig. 2 (A) Optical density (OD) of formazan and Neutral Red obtained after 24 h of BFFs growth in contact with the PNIPAM scaffold and polystyrene multi-well plates without the hydrogel (control). All the data are expressed with the mean ± SE at $n = 16$ and $p < 0.05$. (B) Fluorescence microscopy image of BFFs growth inside the 3D PNIPAM scaffold dyed with Hoescht 33258. The fluorescent points correspond to the cell nuclei at 40 culture days (magnification 10×). Confocal microscopy images of transversal cut of BFFs (GFP) inside the macroporous PNIPAM hydrogel at 40 culture days. (C) Green florescence of transgenic BFFs, (D) Hoechst staining, and (E) the two previous images overlapped. Scale bar: 100 μm.

images (Fig. 2E) corroborate the presence of zones where the cells adhered, grew, and proliferated, and the zones without fluorescence correspond to the matrix walls and empty pores.

It was also demonstrated that the PNIPAM surfaces are biocompatible in contact with bovine fetal fibroblast, showing high cellular adhesion and proliferation after 15 days of culture.[12,25,39] Herein, we demonstrate that the use of this material as a 3D structure for cell growth is also possible. Evidently, the 3D macroporous hydrogel is cytocompatible. Regarding the concave shape of the scaffold pores (non-flat surface), this does not enable the cells to easily adopt their normal morphology (flattened and spindle-shaped morphology) such as that observed on flat surfaces. Even so, it could be demonstrated that the macroporosity of the scaffold material allows cell proliferation since this structure of interconnected macropores not only allows the free flow of waste molecules and nutrients but also the cell migration inside the material. This behaviour is observed from the first day to more than 70 days of culture. This proliferative capacity over time is a desired feature in the development of biomaterials.

### Physicochemical and mechanical properties of the 3D macroporous PNIPAM scaffold before and during cell proliferation

Previous researches have demonstrated that the maximum swelling capacity and equilibrium swelling capacity (% Sw(eq)) of the hydrogels depend on medium properties such as ionic force, pH, temperature, porosity, and cross-linking density. For example, the % Sw(eq) of non-porous (molecular porosity) PNIPAM was reported as 2600% in water and 941% in DMEM culture medium at 25 °C, while at 37 °C (culture condition), the % Sw(eq) decreases to 89% in both the mediums.[12] On the other hand, the % Sw(eq) of the macroporous PNIPAM hydrogel in water is 1900% at 25 °C,[25] which is rather less than that in the non-porous PNIPAM. The swelling capacity must not only be strongly dependent on the solvent and environment temperature but also dependent of the matrix morphology.

It is known that these properties are directly related to the physicochemical and viscoelastic capacity of the hydrogel. Therefore, and according to the mentioned precedents, we think that the swelling capacity as well as mechanical properties

 

of the seeded scaffold could change as the culture days pass. Therefore, both properties were observed during several culture days. Keeping the scaffold culture conditions constant (swollen in DMEM/FBS at 37 °C), the possible variations in the physicochemical properties of the matrix due to pH, temperature, and ionic force changes are resisted. The values of % Sw(eq) were determined considering the amount of solvent taken by the matrix in culture conditions. The % Sw(eq) at zero day was calculated after 24 h of swelling in DMEM/FBS. The obtained values of % Sw(eq) are shown in Fig. 3A, where it can be noted that the presence of cell growth inside the matrix does not significantly affect the swelling capacity of the scaffold.

At the same time, the elastic moduli of cylindrical matrices were determined by uniaxial compression during cell proliferation at culture conditions (DMEM/FBS and 37 °C). The elastic modulus value of the scaffold before cell seeding was 280 kPa and after cell seeding begins to decrease at about 40 kPa in the first culture days. This could evidence possible matrix rearrangement[40] or even proteolytic degradation.[3,41] However, the elastic modulus value remained approximately constant at about 20 kPa from 14 to 40 culture days and then increased, thus achieving a value of 36 kPa after 75 culture days. Concurrently, the elastic modulus of the scaffold, at culture conditions but without seeded cells, was also followed during the same culture days and the elastic modulus values were not significantly altered.

A decreasing during the first few days would indicate biodegradation or rearrangement of the soft scaffold. If biodegradation were occurring, this could tend to a total disintegration over time but it does not occur. In addition, the initial sharp fall and recovery of $E$ is a strong evidence of the structural rearrangement of the matrix without biodegradation since the observed $E$ values after 10 culture days are within the normal reported values.[37]

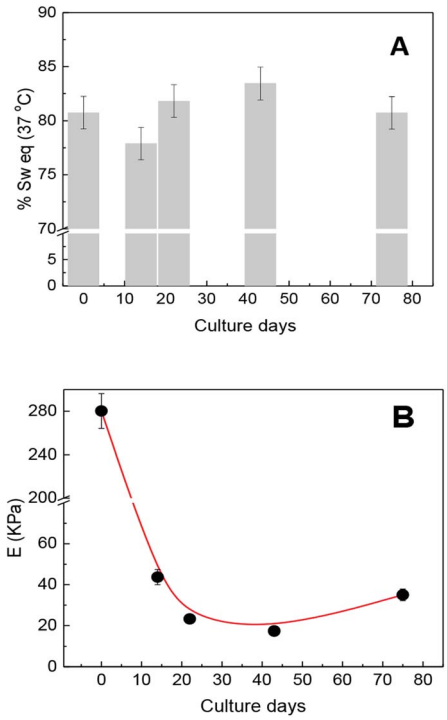


Fig. 3 (A) Maximum swelling capacity (% Sw(eq)) during several culture days. (B) Elastic modulus of the macroporous PNIPAM hydrogel cell seeding at different culture days measured by uniaxial compression in the culture condition.

Although a large number of hydrogels based on biopolymers have been developed for use as 3D scaffolds for tissue engineering, most of them have the disadvantage that they are not able to preserve the mechanical properties for times longer than 30 days of culture[39,42] and in some cases, the cell cannot adhere without the presence of anchorage molecules such as RGD.[40,43]

The ECM protein deposition such as fibronectin and collagen by BFF not only favours cell adhesion on the scaffold but also reinforces the pore. These proteins contain a sequence of amino acids such as proline, hydroxyproline, and glycine that leave exposed N–H and O–H groups capable of interacting through hydrogen bonding with functional groups of the hydrogel matrix (C=O and N–H). This kind of strong bonding could also increase the rigidity of the cell–matrix system.

In addition, the mechanical properties of only cells also could be considered. The growing cell could increase the $E$ of the 3D system but it will depend on the live and dead cell number, which change during the culture days and these are very difficult to determine in a 3D scaffold. From Fig. 2C, it can be seen that the cell number increased considerably at 40 culture days but this does not seem to influence $E$ values in the same way. However, after 70 culture days, the small increase in the $E$ value could then be due to greater number of growing cells.

### Collagen production analysed by Picrosirius Red-polarization method (PSR-POL) and degradation of matrix walls

To verify the presence of collagen, Picrosirius Red-polarization method (PSR-POL) or optical microscopy with polarized light was applied. This technique relies on the birefringent properties of collagen molecules.[44] Picrosirius Red is an elongated molecule and when it is bound parallel to collagen fibrils, it greatly enhances their natural birefringent, which can be detected under polarized light since they appear in bright zones in sharp contrast with the cell mass or the scaffold matrix that remains dark/black. After several culture days, the PNIPAM matrix was labelled with Picrosirius Red in order to detect different kinds of produced collagen. Fig. 4A and B shows the optical images of the same zone of macroporous PNIPAM matrix without (Fig. 4A) and with polarized light (Fig. 4B) at 75 culture days. The bright zone observed in Fig. 4B indicates the presence of collagen in the inner layer of the pore walls since the non-polarized image of the hydrogel wall coincides with the polarized microscopic image.

Therefore, the presence of collagen inside the hydrogel indicates that this was secreted by the cells and can be demonstrated by this assay.

In addition, Fig. 4C–G shows the images of polarized light optical microscopy corresponding to the synthesized fibrillar collagen after 40 and 75 culture days.

Comparing Fig. 4C with Fig. 4E, we can observe that the size of the fibrillar collagen structure considerably increases with culture days and green, yellow, and red zones could be detected

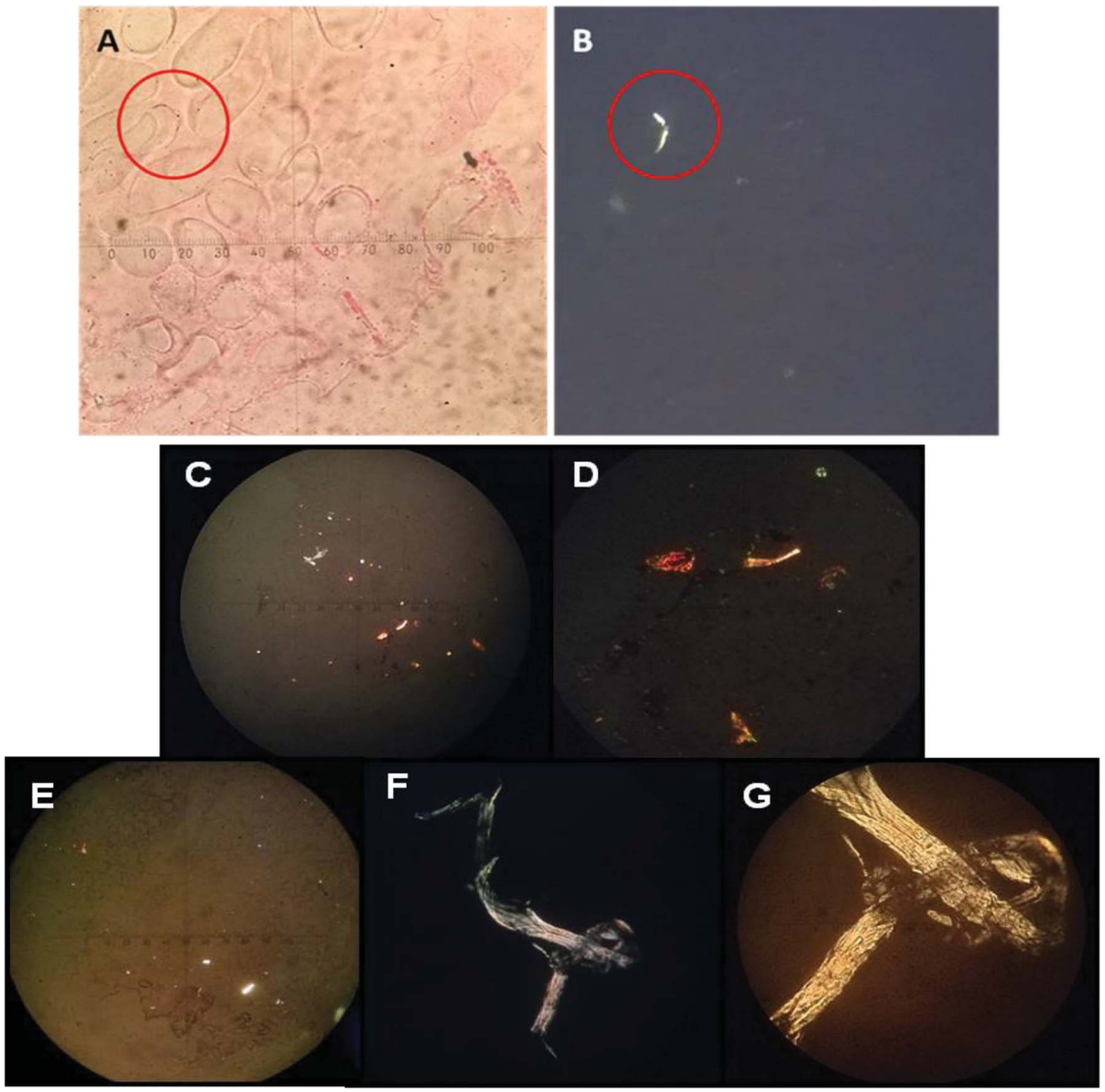


Fig. 4 Microscopic images of FFB cells growing inside macroporous PNIPAM hydrogel in 75 culture days by picrosirius polarization (PSR-POL) method. Magnification: 40×. The red circle indicates a hydrogel without polarization of light (A) and the same polarized image shows the bright zone due to the presence of collagen (B). Collagen production by FFB cells in 3D PNIPAM matrix at different culture days by Picrosirius Red polarization (PSR-POL) method: (C) 40 days, magnification: 10×, (D) 40 days, magnification: 40×, (E) 75 days, magnification: 10×, (F) 75 days, magnification: 40×, (G) 75 days, magnification: 100×.

(Fig. 4F and G). Different colours indicate different collagen thicknesses.[45]

Without polarization, Picrosirius Red-stained hydrogel appears pink-red, all areas are stained, including cellular structures even if they do not contain collagen proteins.[44] In this way, the samples stained with Picrosirius Red can be analysed by bright-field microscopy. Fig. 5 shows the images at 22 and 75 culture days where the empty colourless pores and pink-red hydrogel matrix can be observed. Therefore, the dyed matrix indicates cell growth took place on those zones. In addition, it is possible to observe at 75 days pores with bigger sizes, thus reinforcing the theory of a possible structural relaxation of the viscoelastic matrix during cell growth and proliferation.

### Evaluation of cell morphology and adhesion

Observing the PNIPAM scaffold after 75 culture days by confocal and bright-field optical microscopy, it is possible to confirm that BFF cells mainly adhered on hydrogel walls. The cell morphology can be clearly seen in confocal image taken at first culture days before scaffold is invaded by cell growth. In Fig. 6 can be observed that cells, at 14 culture days, tend to adopt the apparently flattened and spindle-shaped cell morphology. Although, hydrogel pore walls are concave, the viscoelasticity of the material allows that the cells to adopt their normal morphology in contact with the material.

 

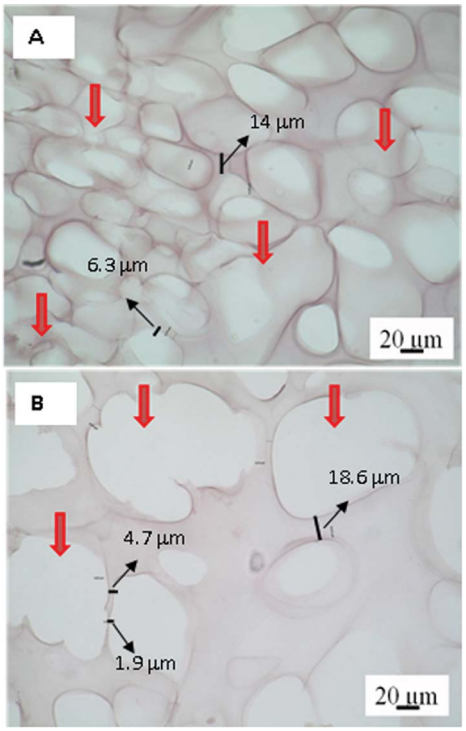


Fig. 5 Images of bright-field optical microscopy for the PNIPAM matrix after 22 (A) and 75 (B) culture days. Red arrows indicate the size pore differents. Scale bar: 20 μm.

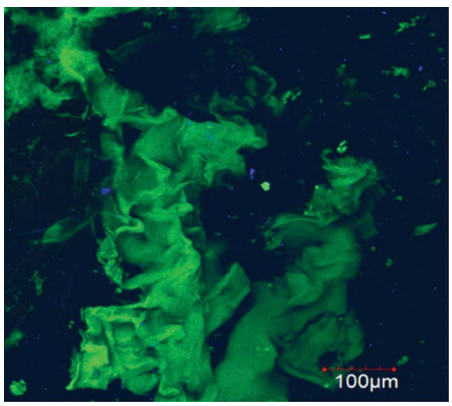


Fig. 6 Confocal microscopy images of BFFs (GFP) inside the macroporous PNIPAM hydrogel at 14 culture days. Scale bar: 100 μm.

## Conclusions

The 3D macroporous matrix of the PNIPAM hydrogel with longitudinal and interconnected pores can be easily synthesized by unidirectional cryo-polymerization. The obtained microarchitecture of the scaffold allows the free flow of biological fluids and the cell growth inside it.

The cytotoxicity effect of the matrix was not observed since high viability of BFF cells in contact with PNIPAM was demonstrated during more than 70 culture days.

The elastic modulus values change during the culture days from 280 kPa to 20 kPa during first culture days and then newly increase to 36 kPa in 70 culture days. However, the 3D structure of the scaffold was preserved during all days of proliferation and the elastic modulus seemed to increase. It was demonstrated that this mechanical behaviour is due to structural rearrangement of the soft matrix and collagen production. Both processes favour the rigidity and stability of the 3D scaffold.

Noteworthy, the BFF cells tend to adopt the typically flattened and spindle-shaped morphology but they must overcome the mechanical resistance of the matrix. After time-relaxation of the matrix, the cells seem to proliferate easily inside it.

Therefore, the morphological, mechanical, and biological properties of macroporous PNIPAM make it suitable for use as a 3D scaffold material due to its behaviour and high biocompatibility with BFF cell growth. Collagen production favours the interaction between the cells and PNIPAM maintaining the structural characteristics of the scaffold. The matrix characteristics and mechanical behaviour allow the application of the PNIPAM hydrogel as 3D scaffold for the *in vitro* cell growth in order to implant or replacement a damaged tissue. However, this cell-scaffold system stands out mainly because the PNIPAM hydrogel can maintain cells for 70 culture days without compromising their viability. The biocompatibility of PNIPAM with other cell lines could expand its field of application in biomedical engineering, for example, using it as a scaffold of osteocyte and osteoblast in order to generate *in vitro* bone tissue.

## Conflicts of interest

There are no conflicts to declare.

## Acknowledgements

The authors thank Dr E. Gabriela Sanchis for help with histological assessment and Antonio Feliciano for help with typographical corrections. This work was supported by FONCYT, CONICET, and SECYT-UNRC. R. Rivero and C. Capella thank CONICET for graduate research fellowships. P. Bosch, C. Liaudat, C. Barbero, and C. Rivarola are permanent researchers of CONICET.

## References

1 C. B. Highley, G. D. Prestwich and J. A. Burdick, Recent advances in hyaluronic acid hydrogels for biomedical applications, *Curr. Opin. Biotechnol.*, 2016, **40**, 35–40.
2 S. Naahidi, M. Jafari, M. Logan, Y. Wang, Y. Yuan, H. Bae, B. Dixon and P. Chen, Biocompatibility of hydrogel-based scaffolds for tissue engineering applications, *Biotechnol. Adv.*, 2017, **35**(5), 530–544.
3 C. Loebel, R. L. Mauck and J. A. Burdick, Local nascent protein deposition and remodelling guide mesenchymal stromal cell mechanosensing and fate in three-dimensional hydrogels, *Nat. Mater.*, 2019, **18**(8), 883–891.

4 Z. Sun, S. S. Guo and R. Fässler, Integrin-mediated mechanotransduction, *Int. J. Biochem. Cell Biol.*, 2016, **215**(4), 445.
5 B. Mattiasson, A. Kumar and I. Y. Galeaev, *Macroporous Polymers: Production Properties and Biotechnological/ Biomedical Applications*, CRC Press, 2009.
6 F. Khan, M. Tanaka and S. R. Ahmad, Fabrication of polymeric biomaterials: a strategy for tissue engineering and medical devices, *J. Mater. Chem. B*, 2015, **3**(42), 8224–8249.
7 A. Vedadghavami, F. Minooei, M. H. Mohammadi, S. Khetani, A. Rezaei Kolahchi, S. Mashayekhan and A. Sanati-Nezhad, Manufacturing of hydrogel biomaterials with controlled mechanical properties for tissue engineering applications, *Acta Biomater.*, 2017, **62**, 42–63.
8 V. Agarwal, D. Ho, D. Ho, Y. Galabura, F. Yasin, P. Gong, W. Ye, R. Singh, A. Munshi, M. Saunders, R. C. Woodward, T. St. Pierre, F. M. Wood, M. Fear, D. Lorenser, D. D. Sampson, B. Zdyrko, I. Luzinov, N. M. Smith and K. S. Iyer, Functional Reactive Polymer Electrospun Matrix, *ACS Appl. Mater. Interfaces*, 2016, **8**(7), 4934–4939.
9 V. J. Jijo, K. P. Sharma, R. Mathew, S. Kamble, P. R. Rajamohanan, T. G. Ajithkumar, M. V. Badiger and G. Kumaraswamy, Volume Transition of PNIPAM in a Nonionic Surfactant Hexagonal Mesophase, *Macromolecules*, 2010, **43**(10), 4782–4790.
10 N. Izza Taib, V. Agarwal, N. M. Smith, R. C. Woodward, T. G. St. Pierre and K. S. Iyer, Direct correlation of PNIPAM thermal transition and magnetic resonance relaxation of iron oxide nanoparticles, *Mater. Chem. Front.*, 2017, **1**(11), 2335–2340.
11 S. Shekhar, M. Mukherjee and A. K. Sen, Swelling, thermal and mechanical properties of NIPAM-based terpolymeric hydrogel, *Polym. Bull.*, 2016, **73**(1), 125–145.
12 R. Rivero, F. Alustiza, V. Capella, C. Liaudat, N. Rodriguez, P. Bosch, C. Barbero and C. Rivarola, Physicochemical properties of ionic and non-ionic biocompatible hydrogels in water and cell culture conditions: relation with type of morphologies of bovine fetal fibroblasts in contact with the surfaces, *Colloids Surf., B*, 2017, **158**, 488–497.
13 H. Vihola, A. Laukkanen, L. Valtola, H. Tenhu and J. Hirvonen, Cytotoxicity of thermosensitive polymers poly(*N*-isopropylacrylamide), poly(*N*-vinylcaprolactam) and amphiphilically modified poly(*N*-vinylcaprolactam), *Biomaterials*, 2005, **26**(16), 3055–3064.
14 Y. Lei, C. Fang, L. Tianqing, R. L. Jian, S. Kedong, J. Lili, W. Shuang and G. Wenhua, Comparison of mesenchymal stem cells released from poly(*N*-isopropylacrylamide) copolymer film and by trypsinization, *Biomed. Mater.*, 2012, **7**(3), 035003.
15 M. A. Cooperstein and H. E. Canavan, Assessment of cytotoxicity of (*N*-isopropyl acrylamide) and poly(*N*-isopropyl acrylamide)-coated surfaces, *Biointerphases*, 2013, **8**(1), 19.
16 V. Capella, R. E. Rivero, A. C. Liaudat, L. E. Ibarra, D. A. Roma, F. Alustiza, F. Mañas, C. A. Barbero, P. Bosch, C. R. Rivarola and N. Rodriguez, Cytotoxicity and bioadhesive properties of poly-*N*-isopropylacrylamide hydrogel, *Heliyon*, 2019, **5**(4), e01474.
17 K. S. Anseth, C. N. Bowman and L. Brannon-Peppas, Mechanical properties of hydrogels and their experimental determination, *Biomaterials*, 1996, **17**(17), 1647–1657.
18 A. Vedadghavami, F. Minooei, M. H. Mohammadi, S. Khetani, A. Rezaei Kolahchi, S. Mashayekhan and A. Sanati-Nezhad, Manufacturing of hydrogel biomaterials with controlled mechanical properties for tissue engineering applications, *Acta Biomater.*, 2017, **62**(suppl. C), 42–63.
19 M. A. Haq, Y. Su and D. Wang, Mechanical properties of PNIPAM based hydrogels: a review, *Mater. Sci. Eng. C*, 2017, **70**, 842–855.
20 M. V. Martínez, S. Bongiovanni Abel, R. Rivero, M. C. Miras, C. R. Rivarola and C. A. Barbero, Polymeric nanocomposites made of a conductive polymer and a thermosensitive hydrogel: strong effect of the preparation procedure on the properties, *Polymer*, 2015, **78**, 94–103.
21 R. E. Rivero, M. A. Molina, C. R. Rivarola and C. A. Barbero, Pressure and microwave sensors/actuators based on smart hydrogel/conductive polymer nanocomposite, *Sens. Actuators, B*, 2014, **190**, 270–278.
22 M. Zhong, Y.-T. Liu and X.-M. Xie, Self-healable, super tough graphene oxide-poly(acrylic acid) nanocomposite hydrogels facilitated by dual cross-linking effects through dynamic ionic interactions, *J. Mater. Chem. B*, 2015, **3**(19), 4001–4008.
23 Y. Zhang, Y. Li and W. Liu, Dipole–Dipole and H-Bonding Interactions Significantly Enhance the Multifaceted Mechanical Properties of Thermoresponsive Shape Memory Hydrogels, *Adv. Funct. Mater.*, 2015, **25**(3), 471–480.
24 L. Santos, G. Fuhrmann, M. Juenet, N. Amdursky, C.-M. Horejs, P. Campagnolo and M. M. Stevens, Extracellular Stiffness Modulates the Expression of Functional Proteins and Growth Factors in Endothelial Cells, *Adv. Healthcare Mater.*, 2015, **4**(14), 2056–2063.
25 R. E. Rivero, F. Alustiza, N. Rodríguez, P. Bosch, M. C. Miras, C. R. Rivarola and C. A. Barbero, Effect of functional groups on physicochemical and mechanical behavior of biocompatible macroporous hydrogels, *React. Funct. Polym.*, 2015, **97**, 77–85.
26 S. Tang, H. Ma, H.-C. Tu, H.-R. Wang, P.-C. Lin and K. S. Anseth, Adaptable Fast Relaxing Boronate-Based Hydrogels for Probing Cell–Matrix Interactions, *Adv. Sci.*, 2018, **5**(9), 1800638.
27 T. M. A. Henderson, K. Ladewig, D. N. Haylock, K. M. McLean and A. J. O'Connor, Cryogels for biomedical applications, *J. Mater. Chem. B*, 2013, **1**(21), 2682–2695.
28 D. R. Askeland, P. P. Fulay and W. J. Wright, *The Science and Engineering of Materials*, SI edn, Cengage Learning, 2011.
29 F. Topuz and O. Okay, Macroporous hydrogel beads of high toughness and superfast responsivity, *React. Funct. Polym.*, 2009, **69**(5), 273–280.
30 M. Nowak-Imialek, W. A. Kues, B. Petersen, A. Lucas-Hahn, D. Herrmann, S. Haridoss, M. Oropeza, E. Lemme, H. R. Schöler, J. W. Carnwath and H. Niemann, Oct4-Enhanced Green Fluorescent Protein Transgenic Pigs: A

 

New Large Animal Model for Reprogramming Studies, *Stem Cells Dev.*, 2011, **20**(9), 1563–1575.

31 D. W. Hutmacher, T. Schantz, I. Zein, K. W. Ng, S. H. Teoh and K. C. Tan, Mechanical properties and cell cultural response of polycaprolactone scaffolds designed and fabricated *via* fused deposition modeling, *J. Biomed. Mater. Res., Part A*, 2001, **55**(2), 203–216.

32 G. Fotakis and J. A. Timbrell, In vitro cytotoxicity assays: Comparison of LDH, neutral red, MTT and protein assay in hepatoma cell lines following exposure to cadmium chloride, *Toxicol. Lett.*, 2006, **160**(2), 171–177.

33 G. Repetto, A. del Peso and J. L. Zurita, Neutral red uptake assay for the estimation of cell viability/cytotoxicity, *Nat. Protoc.*, 2008, **3**, 1125.

34 G. Ates, T. Vanhaecke, V. Rogiers and R. M. Rodrigues, Assaying Cellular Viability Using the Neutral Red Uptake Assay, in *Cell Viability Assays: Methods and Protocols*, ed. D. F. Gilbert and O. Friedrich, Springer New York, New York, NY, 2017, pp. 19–26.

35 P.-Y. Chen, K.-C. Yang, C.-C. Wu, J.-H. Yu, F.-H. Lin and J.-S. Sun, Fabrication of large perfusable macroporous cell-laden hydrogel scaffolds using microbial transglutaminase, *Acta Biomater.*, 2014, **10**(2), 912–920.

36 L. C. U. Junqueira, G. Bignolas and R. R. Brentani, Picrosirius staining plus polarization microscopy, a specific method for collagen detection in tissue sections, *Histochem. J.*, 1979, **11**(4), 447–455.

37 P. X. Ma and R. Zhang, Microtubular architecture of biodegradable polymer scaffolds, *J. Biomed. Mater. Res.*, 2001, **56**(4), 469–477.

38 V. M. Gun'ko, L. I. Mikhalovska, I. N. Savina, R. V. Shevchenko, S. L. James, P. E. Tomlins and S. V. Mikhalovsky, Characterisation and performance of hydrogel tissue scaffolds, *Soft Matter*, 2010, **6**(21), 5351–5358.

39 X. Zhao, Q. Lang, L. Yildirimer, Z. Y. Lin, W. Cui, N. Annabi, K. W. Ng, M. R. Dokmeci, A. M. Ghaemmaghami and A. Khademhosseini, Photocrosslinkable Gelatin Hydrogel for Epidermal Tissue Engineering, *Adv. Healthcare Mater.*, 2016, **5**(1), 108–118.

40 T. E. Brown, B. J. Carberry, B. T. Worrell, O. Y. Dudaryeva, M. K. McBride, C. N. Bowman and K. S. Anseth, Photopolymerized dynamic hydrogels with tunable viscoelastic properties through thioester exchange, *Biomaterials*, 2018, **178**, 496–503.

41 K. M. Schultz, K. A. Kyburz and K. S. Anseth, Measuring dynamic cell–material interactions and remodeling during 3D human mesenchymal stem cell migration in hydrogels, *Proc. Natl. Acad. Sci.*, 2015, **112**(29), E3757–E3764.

42 A. Grigore, B. Sarker, B. Fabry, A. R. Boccaccini and R. Detsch, Behavior of Encapsulated MG-63 Cells in RGD and Gelatine-Modified Alginate Hydrogels, *Tissue Eng., Part A*, 2014, **20**(15–16), 2140–2150.

43 H. W. Ooi, C. Mota, A. T. ten Cate, A. Calore, L. Moroni and M. B. Baker, Thiol–Ene Alginate Hydrogels as Versatile Bioinks for Bioprinting, *Biomacromolecules*, 2018, **19**(8), 3390–3400.

44 L. Rittié, Method for Picrosirius Red-Polarization Detection of Collagen Fibers in Tissue Sections, in *Fibrosis: Methods and Protocols*, ed. L. Rittié, Springer New York, New York, NY, 2017, pp. 395–407.

45 L. C. U. Junqueira, G. S. Montes and E. M. Sanchez, The influence of tissue section thickness on the study of collagen by the Picrosirius-polarization method, *Histochemistry*, 1982, **74**(1), 153–156.